Chemical Science

ROYAL SOCIETY OF CHEMISTRY

EDGE ARTICLE

View Article Online
View Journal | View Issue

Cite this: *Chem. Sci.*, 2023, **14**, 13979

All publication charges for this article have been paid for by the Royal Society of Chemistry

Received 24th October 2023
Accepted 21st November 2023

DOI: 10.1039/d3sc05677e

rsc.li/chemical-science

Chiral cobalt(II) complex-promoted asymmetric *para*-Claisen rearrangement of allyl α-naphthol ethers†

Hongkun Zeng, Lifeng Wang, Zhishan Su, Meijia Ying, Lili Lin * and Xiaoming Feng *

Due to experiencing a challenging dearomatization process, the aromatic sigmatropic rearrangement of allyl naphthyl ethers is a difficult yet efficient method to build useful naphthalenone skeletons. Here, we report a *para*-Claisen rearrangement-based asymmetric dearomatization of allyl α-naphthol ethers enabled by a *N*,*N*′-dioxide/Co^{II} complex. A variety of naphthalenones were obtained in moderate to good yields with good to excellent ee values. Interestingly, by exchanging the allyl group on the ether and that at the *para*-position of the benzene ring, enantiodivergent synthesis can be achieved. Experimental studies and DFT calculations revealed that aryl allyl ethers tend to transform *via* a stepwise allyl π-complex migration pathway, while, alkyl allyl ethers transformed through a concerted *ortho*-Claisen rearrangement/Cope rearrangement sequence.

Introduction

The chiral naphthalenone skeleton is widely found in natural products and fungal species (Scheme 1a).[1] For example, *pereniporins* A, isolated from a fungus *Perenniporia* sp. inhabiting the larva of *Euops chinesis*, shows significant antifungal activity against multiple plant pathogens.[2] (+)-*Rishirilides* B, isolated from the culture broth of *Streptomyces* strain, *Streptomyces rishiriensis* OFR-1056, can effectively inhibit plasma α_2-macroglobulin.[3] (−)-5-Hydroxy-4-methoxy-1-tetralone was isolated from the roots of *Engelhardia roxburghiana*, exhibiting antitubercular activity.[4] These compounds all have a naphthalenone skeleton and possess a chiral centre at the C4-position.

Asymmetric dearomatization of naphthol derivatives is an efficient method to build chiral naphthalenone skeletons.[5] However, compared to well-established oxidative[6] or transition metal mediated[7] dearomatizations, rearrangement-based[8] dearomatizations are relatively less explored. The aromatic [*n*,*m*]-sigmatropic rearrangement of allyl or propargyl naphthyl ethers can rapidly construct allyl or propargyl functionalized naphthalenones.[9] Bandini developed a gold-catalyzed dearomatization of 2-naphthols with alkynes, and an enantioselective investigation afforded chiral dihydrofurylnaphthalen-2(1*H*)-one in 81% yield with 65% ee.[10] Recently, our group reported a thermal [3,3]-sigmatropic rearrangement of naphthyl 1-propargyl ethers, and the enantioselective version was achieved by a chiral cobalt catalysis at 70 °C.[11] For the

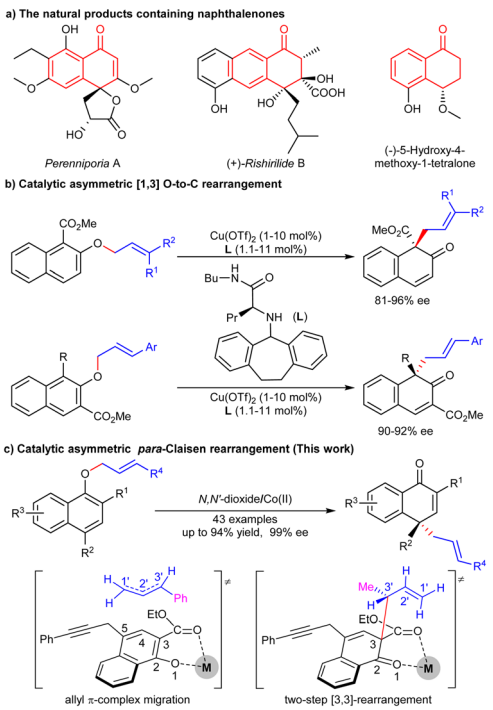

Scheme 1 Catalytic asymmetric rearrangements of allyl naphthyl ethers.

Key Laboratory of Green Chemistry & Technology, Ministry of Education, College of Chemistry, Sichuan University, Chengdu 610064, China. E-mail: lililin@scu.edu.cn; xmfeng@scu.edu.cn

† Electronic supplementary information (ESI) available: ^{1}H, $^{13}C\{^{1}H\}$ and $^{19}F\{^{1}H\}$ NMR, HPLC spectra (PDF). X-ray crystallographic data for **B1** and **B35**. CCDC 2289879 and 2235350. For ESI and crystallographic data in CIF or other electronic format see DOI: https://doi.org/10.1039/d3sc05677e

rearrangement of allyl naphthol ethers, Ishihara and Yao used a chiral α-amino amide/Cu(II) catalyst to achieve the asymmetric [1,3] O-to-C dearomative rearrangement of alkyl 2-allyloxy-1/3-naphthoates (Scheme 1b).[12] If allyl α-naphthol ethers were applied, *ortho*-Claisen/Cope rearrangement or an allyl π-complex migration process will occur,[13] achieving *para*-Claisen rearrangement.[14] The difficulty lies in the remote enantioselective control.

Considering that the catalytic asymmetric rearrangement-based dearomatizations are limited and further research is necessary, herein, we report a chiral cobalt(II)/*N*,*N*′-dioxide complex-promoted asymmetric *para*-Claisen rearrangement of allyl α-naphthol ethers. A variety of chiral naphthalenones bearing a chiral all-carbon quaternary centre were obtained in good yields with excellent ee values under mild conditions (Scheme 1c).

Results and discussion

At the outset, ethyl 1-(cinnamyloxy)-4-propargyl-2-naphthoate **A1** was selected as the model substrate to optimize the reaction conditions (Table 1). First, various chiral *N*,*N*′-dioxide ligands were evaluated by complexing with $Co(BF_4)_2\cdot 6H_2O$ in 1,1,2,2-TCE at 10 °C. It was found that the chiral skeleton affected greatly the reactivity. L-Proline derived **L_3-PrPr$_2$**, L-pipecolic acid derived **L_3-PiPr$_2$** and L-ramipril-derived **L_3-RaPr$_2$** gave very low yields albeit with moderate enantioselectivity, while (*S*)-tetrahydroisoquinoline-3-carboxylic acid-derived **L_3-TQPh** could give 73% yield with 74% ee (entries 1–4). The amide moiety in the ligand, generally shielding one of the faces of prochiral substrates, also played a very important role in enantioselectivity. Switching the substituent of the amide moiety from rigid phenyl to the flexible cyclohexyl led to better yield and enantioselectivity (entry 5, 78% yield, 82% ee). When the substituent of amide was the isopropyl or cyclopropyl group, the reactivity and selectivity were further improved (entries 6–7). When the temperature was raised to 35 °C, the substrate decomposed and enantioselectivity decreased (entry 8). The solvent affected the reaction greatly. Altering 1,1,2,2-TCE to CH_2Cl_2 resulted in a decreased enantioselectivity (69% ee, entry 9). When THF was used as the solvent, no reaction occurred (entry 10), which might be attributed to the competitive coordination with the catalyst between the solvent and substrate. Examination of different metal salts by complexing with **L_3-TQCp** showed that $Co(OTf)_2$, $Zn(OTf)_2$ and $Mg(OTf)_2$ could also promote the reaction, and the enantioselectivities decreased a little (entries 11–13).

With the optimized reaction conditions in hand (Table 1, entry 7), the substrate scope was explored. As illustrated in Scheme 2, the bulkier ester group was favorable for the enantioselectivity (**B1–B4**). Methyl ester reduced the ee value to 81%, while isopropyl ester and phenyl ester increased the enantioselectivity to 97% ee. A gram-scale synthesis of **B1** by applying 3 mmol **A1** furnished smoothly 1.25 g of the desired product **B1** in 93% yield with 91% ee. In the absence of an ester group or when the ester group (R1) was altered to others (**A41–A45**), such as amide and CN, no reaction occurred. When the ester group was altered to the aldehyde or ketone group, the reaction mixture was complex, or the enantioselectivity was very low. The results demonstrated the importance of the ester group (R1), whose roles might be that the coordination ability of the ester group helped the substrates to coordinate with the catalyst in a tight bidentate manner, facilitating the C–O bond cleavage to undergo the rearrangement process, and also fixing the substrate to benefit the enantioselective control. In addition, the electron-withdrawing properties of the ester group might also be helpful for the stabilization of the transition state. Propargyl (**A5**), methyl ethyl ether (**A6**), benzyl (**A7**), halide (Cl, **A8**) and propyl (**A9**) groups were well tolerated on the *para*-position of allyl α-naphthol ether, affording the desired products **B5–B9** in moderate to high yields with excellent ee values. When the cyclopropyl group (**A10**) or methyl ester (**A11**) was on the *para*-position, the reactivity and enantioselectivity decreased (**B10** and **B11**). **A12** with the ethoxy group transformed in only 30% yield with 5% ee. The substitution at the

Table 1 Optimization of the reaction conditions[a]

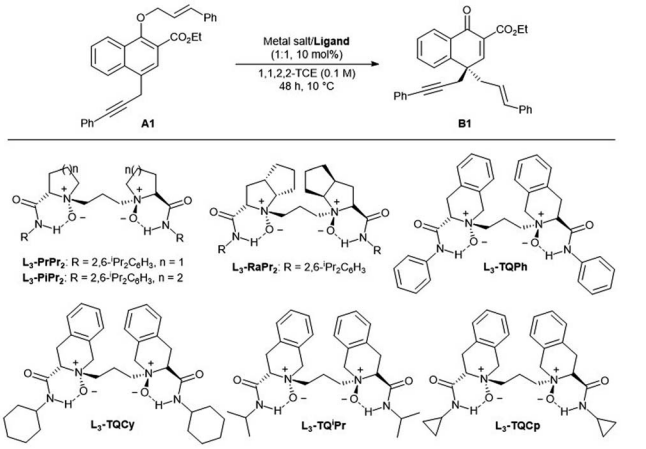

Entry	Ligand	Metal salt	Yield[b] [%]	ee[c] [%]
1	**L_3-PrPr$_2$**	$Co(BF_4)_2\cdot 6H_2O$	<5	63
2	**L_3-PiPr$_2$**	$Co(BF_4)_2\cdot 6H_2O$	13	57
3	**L_3-RaPr$_2$**	$Co(BF_4)_2\cdot 6H_2O$	<5	55
4	**L_3-TQPh**	$Co(BF_4)_2\cdot 6H_2O$	73	74
5	**L_3-TQCy**	$Co(BF_4)_2\cdot 6H_2O$	78	82
6	**L_3-TQ^{i}Pr**	$Co(BF_4)_2\cdot 6H_2O$	87	85
7	**L_3-TQCp**	$Co(BF_4)_2\cdot 6H_2O$	86	92
8[d]	**L_3-TQCp**	$Co(BF_4)_2\cdot 6H_2O$	<5	36
9[e]	**L_3-TQCp**	$Co(BF_4)_2\cdot 6H_2O$	83	69
10[f]	**L_3-TQCp**	$Co(BF_4)_2\cdot 6H_2O$	NR	—
11	**L_3-TQCp**	$Co(OTf)_2$	83	86
12	**L_3-TQCp**	$Zn(OTf)_2$	89	85
13	**L_3-TQCp**	$Mg(OTf)_2$	90	89

[a] Unless otherwise noted, all reactions were carried out with **A1** (0.05 mmol) and ligand/metal salt (1 : 1, 10 mol%) in 1,1,2,2-TCE (0.1 M) at 10 °C for 48 h without the protection of inert gas. [b] Yield of the isolated product. [c] Determined by HPLC analysis on a chiral stationary phase. [d] At 35 °C. [e] CH_2Cl_2 (0.5 ml) as solvent. [f] THF (0.5 ml) as solvent. 1,1,2,2-TCE = 1,1,2,2-tetrachloroethane. NR = no reaction.

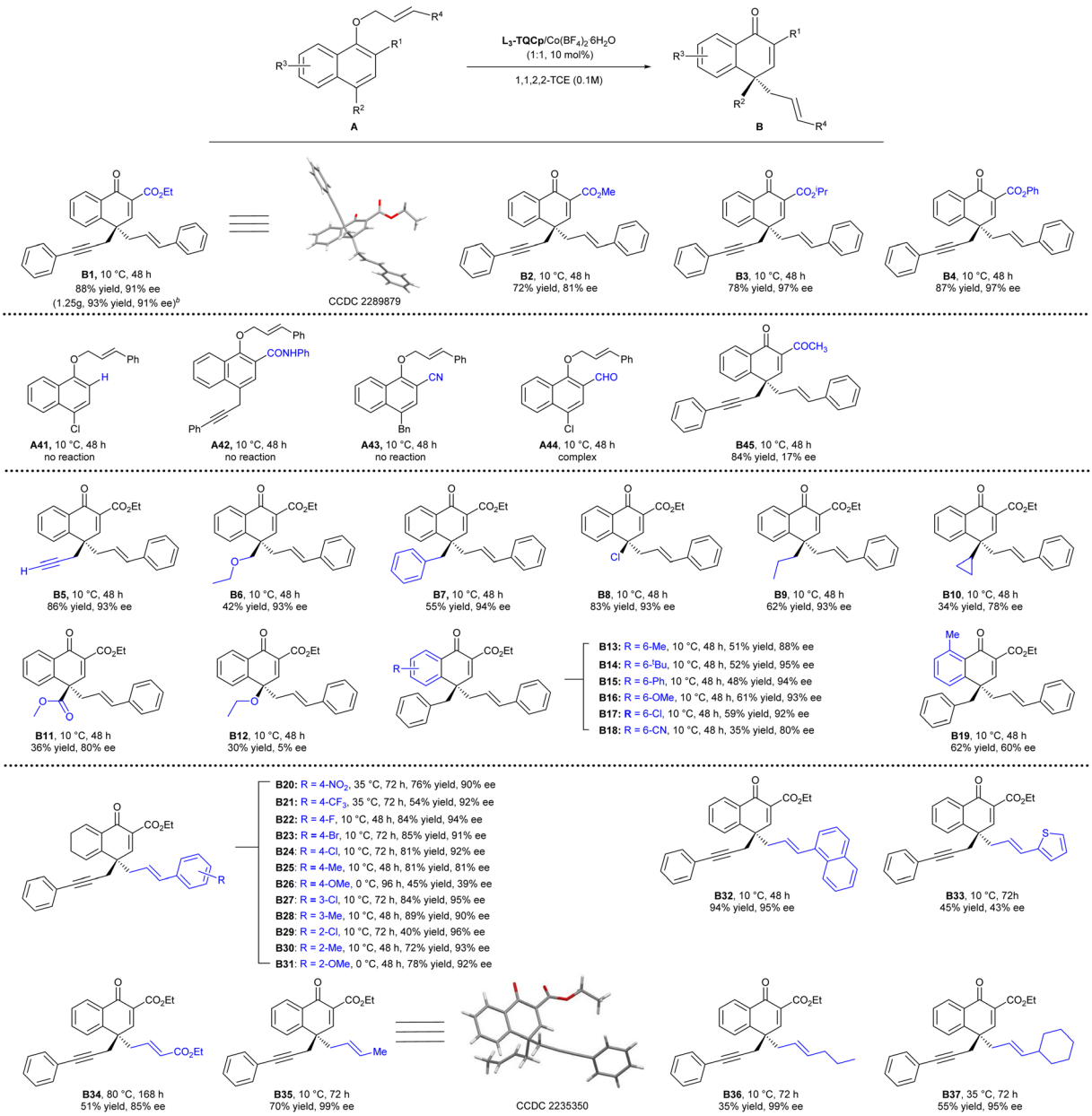

Scheme 2 Substrate scope[a]. [a] Unless otherwise noted, all reactions were carried out with **A** (0.1 mmol) and **L$_3$-TQCp**/Co(BF$_4$)$_2$·6H$_2$O (1 : 1, 10 mol%) in 1,1,2,2-TCE (0.1 M). Yields of the isolated product. ee was determined by HPLC or UPC^2 analysis on a chiral stationary phase. [b] 3.0 mmol **A1** was used.

naphthyl ring was also investigated. Electron-donating groups, such as Me, OMe, Ph, *t*-Bu, even halogen Cl at the 6-position had no obvious effect on the yield and enantioselectivity (**B13–B17**). The electron-withdrawing group (CN) decreased the enantioselectivity (80% ee, **B18**). Furthermore, introducing a methyl group at the 8-position resulted in a reduced ee value (60% ee, **B19**), possibly due to the larger steric hindrance.

A range of aryl allyl bearing either electron-donating or electron-withdrawing groups at the *ortho*, *meta*, or *para* position of the arene moiety were also examined. Substrates with electron-withdrawing groups at the *para*-position transformed in good yields with excellent enantioselectivities (**B20–B24**, 54–85% yield, 90–94% ee). The enantioselectivities decreased when electron-donating groups were at the *para*-position (**B25**, **B26**, 39–81% ee), which might be caused by a stronger background reaction due to the higher reactivity of substrates. The low yield of **B26** was caused by the decomposition of **A26** under the reaction conditions. Substitutes at the *ortho* or *meta* position had a little impact on the enantioselectivity, and all the tested substrates yielded the desired products with excellent ee values (**B27–B31**).

The 1-naphthyl allyl substrate transformed into the product **B32** in 94% yield with 95% ee. Product **B33** with the allyl heteroarene group was obtained in moderate yield with a moderate ee value. Moreover, unactivated allyl groups were also suitable in the asymmetric *para*-Claisen rearrangement. Ethyl but-2-

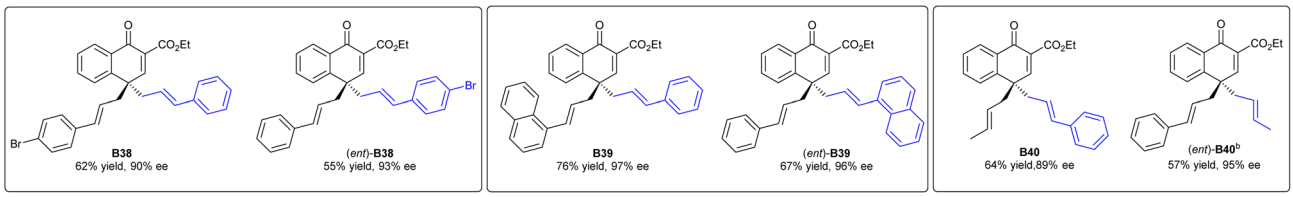

Scheme 3 Substrate-controlled enantiodivergent synthesis[a]. [a] Unless otherwise noted, all reactions were carried out with **A** (0.1 mmol) and **L$_3$-TQCp**/Co(BF$_4$)$_2$·6H$_2$O (1 : 1, 10 mol%) in 1,1,2,2-TCE (0.1 M), at 10 °C for 48 h. Yields of the isolated product. ee was determined by HPLC analysis on a chiral stationary phase. [b] At 20 °C.

enoate-substituted allylic ether **A34** bearing an ester moiety transformed into the targeted product **B34** in 51% yield with 85% ee. **A35**, **A36** and **A37** with aliphatic functional groups, furnishing the desired products **B35–B37** in excellent ee values (95–99% ee) albeit with moderate yields. The absolute configurations of the products **B1** and **B35** were determined to be (*R*) by X-ray crystallography analysis.

para-Allyl substrates were compatible in the present system, giving the desired products **B38**, **B39**, and **B40** in excellent ee values. Interestingly, their enantiomers (*ent*)-**B38**, (*ent*)-**B39** and (*ent*)-**B40** could be obtained with the same ee values by exchanging the allyl group on the ethers and that at the C4-position, which gave an interesting entry to enantiodivergent synthesis (Scheme 3).

To gain insight into the mechanism, the relationship between the enantiomeric excess of the product and catalyst was studied. As shown in Fig. 1a, a clear linearity was observed, indicating that the species formed by the coordination of Co^{II} and the chiral *N*,*N*′-dioxide ligand in a 1 : 1 ratio might be the catalytically active species. In addition, the kinetic studies showed a first-order kinetic dependence on the chiral **L$_3$-TQCp**/Co(BF$_4$)$_2$·6H$_2$O catalyst and **A1** (Fig. 1b). A crossover experiment was conducted using **A8** and **A32** as substrates (Fig. 1c). Products **B8** and **B32** were obtained under Lewis acid accelerated or thermal mediated conditions, and crossover products were not observed. Both kinetic studies and crossover experiment indicated that the rearrangement might involve an intramolecular reaction.

In addition, to illustrate the rearrangement pathway, a density functional theory (DFT) study was performed at the B3LYP-D3/6-31G(d,p) (SMD, CCl_4) level of theory with Zn(OTf)$_2$ as the catalyst because Zn(II) gave similar results to Co(II), meanwhile reducing the computational difficulty (Fig. 2). It was revealed that the conversion from **IM1-Ph** to **IM4-Ph** involved an allyl π-complex migration mechanism (Fig. 2a). A tight ion-pair intermediate (**IM2-Ph**) was formed *via* the transition state **TS1-Ph**, accompanied by the cleavage of the C1′–O bond. The $\Delta G^{\neq}$ in this step was 8.6 kcal mol^{-1}. Then, **IM2-Ph** underwent a conformation change and transformed into a more stable intermediate **IM3-Ph**. In the following step, the C1′–C5 bond in **IM4-Ph** was constructed through ion-pair coupling *via* **TS2-Ph**, with a $\Delta G^{\neq}$ of only 1.3 kcal mol^{-1}. For comparison, we also studied the C3–C3′ coupling *via* **TS2-Ph-a**. The $\Delta G^{\neq}$ of **TS2-Ph-a** was 1.3 kcal mol^{-1} less stable than that of **TS2-Ph**, indicating that the cation fragment preferred to interact with the C5 atom of the Zn(II)-coordinated anion for **IM4-Ph**.

Comparatively, when the alkyl Me group replaces the aryl Ph group that can stabilize allyl cations, the conversion from **IM1-Me** to **IM3-Me** involved sequential *ortho*-Claisen rearrangement/Cope rearrangement (Fig. 2b). During these processes, two six-membered ring transition states (**TS1-Me** and **TS2-Me**) were

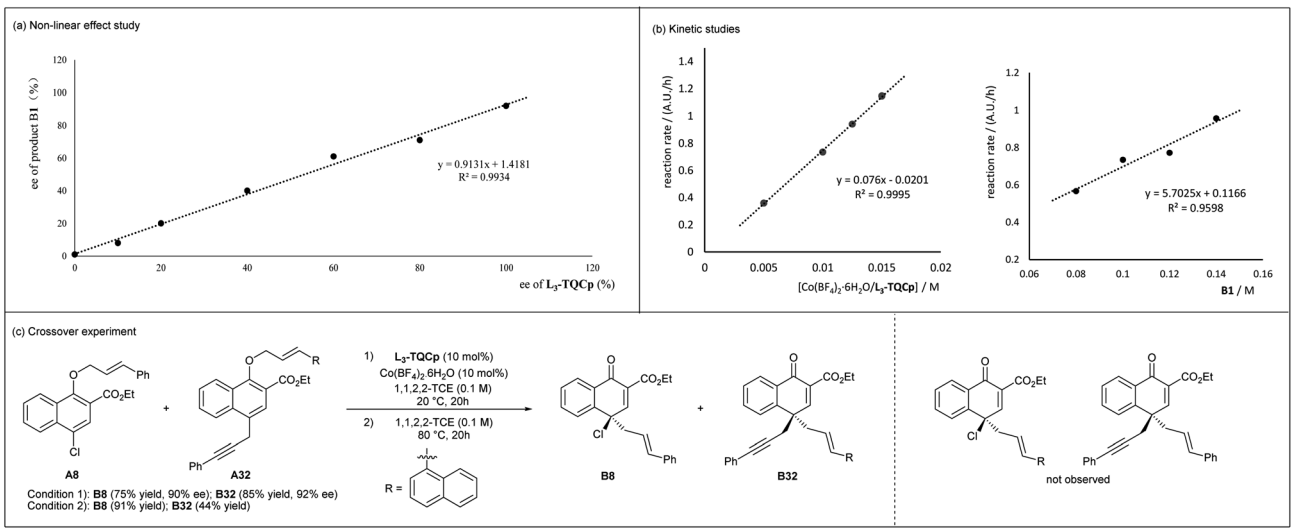

Fig. 1 Exploration on the mechanism.

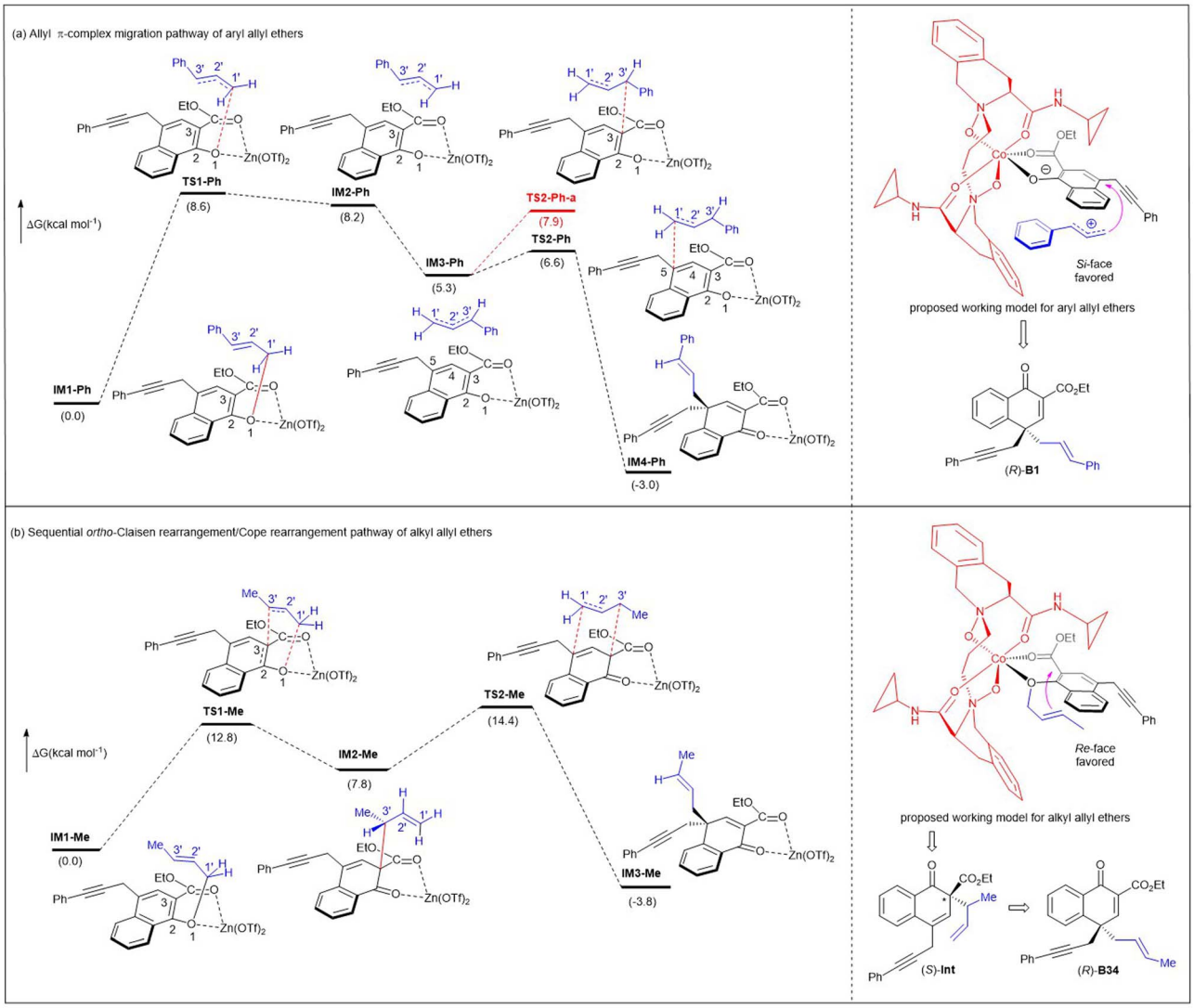

Fig. 2 DFT calculations on rearrangement pathways and proposed asymmetric induction models for both aryl and alkyl allyl ethers.

generated, with the activation barriers of 12.8 kcal mol^{-1} and 6.6 kcal mol^{-1}, respectively. The reaction was exergonic by 3.8 kcal mol^{-1}. The energy barrier associated with the formation of ion-pair coupling was evaluated by a relaxed scan of the C1′–O bond in **IM1-Me′** (from 1.502 to 3.022 Å). The corresponding $\Delta E^{\neq}$ was 20.7 kcal mol^{-1} (see Fig. S5 in ESI† for more details).

In addition, combining our previous studies on *N*,*N*′-dioxide/metal catalysis,[15,16] we proposed two catalytic modes to explain the stereochemistry of the reaction. Chiral *N*,*N*′-dioxide and naphthyl 1-allyl ether coordinated to Co(II) in tetradentate and bidentate fashions, respectively, to form a slightly distorted hexahedral complex. Aryl allyl ether **A1** converts to a tight ion-pair intermediate with the assistance of the *N*,*N*′-dioxide/Co(II) complex. Since the *Re*-face of the enolate anion is shielded by the amide moiety of the ligand, the allyl cation attacks from its *Si*-face to give (*R*)-**B1**. For alkyl allyl ether **A35**, the allyl unit faces to the right-bottom with less steric hindrance, so it tends to approach the enolate ether from the *Re*-face, undergoing an *ortho*-Claisen rearrangement to generate the chiral (*S*)-**Int**, and then undergoing rapid Cope rearrangement to provide more stable (*R*)-**B35**.

Conclusions

In summary, we have successfully developed an efficient catalytic asymmetric *para*-Claisen rearrangement of naphthyl 1-allyl ethers by using a chiral *N*,*N*′-dioxide/Co(II) complex as the catalyst, providing a facile and efficient route to synthesize valuable naphthalenones with a chiral center at the C4-position under mild reaction conditions. Notably, exchanging the allyl groups at the *para*-position and on the ethers, substrate-controlled enantiodivergent synthesis can be achieved. DFT calculations revealed that aryl allyl ethers that can stabilize allyl cations tend to experience an allyl π-complex migration process, while alkyl allyl ethers involve concerted *ortho*-Claisen rearrangement/Cope rearrangement sequence processes.

Data availability

Further details of the experimental procedure, ^{1}H, ^{13}C{^{1}H} and ^{19}F{^{1}H} NMR, HPLC spectra and X-ray crystallographic data are available in the ESI.†

Author contributions

H. K. Z. preformed the experiments. M. J. Y. repeated the data. Z. S. S. conducted the DFT calculation. X. M. F., L. L. L. and L. F. W. supervised the project. H. K. Z. and L. L. L. co-wrote the manuscript.

Conflicts of interest

There are no conflicts to declare.

Acknowledgements

We appreciate the National Natural Science Foundation of China (no. 22171189 and 22188101), Sichuan Science and Technology Program (No. 2021YJ0561), and Fundamental Research Funds for the Central Universities for financial support. We are grateful to Dr Yuqiao Zhou from the College of Chemistry, Sichuan University for the X-ray single crystal diffraction analysis.

Notes and references

1 S. R. M. Ibrahim, S. A. Fadil, H. A. Fadil, B. A. Eshmawi, S. G. A. Mohamed and G. A. Mohamed, *Toxins*, 2022, **14**, 154.

2 Y. Feng, L. Wang, S. B. Niu, L. Li, Y. k. Si, X. Z. Liu and Y. S. Che, *J. Nat. Prod.*, 2012, **75**, 1339.

3 H. Iwaki, Y. Nakayama, M. Takahashi, S. Uetsuki, M. Kido and Y. Fukuyama, *J. Antibiot.*, 1984, **37**, 1091.

4 (*a*) W. Y. Liu, C. F. Peng, L. L. Tsai, J. J. Chen, M. J. Cheng and I. S. Chen, *Planta Med.*, 2005, **71**, 171; (*b*) D. Chanda, D. Saikia, J. K. Kumar, J. P. Thakur, J. Agarwal, C. S. Chanotiya, K. Shanker and A. S. Negi, *Bioorg. Med. Chem. Lett.*, 2011, **21**, 3966.

5 For reviews, see: (*a*) C. X. Zhuo, C. Zheng and S. L. You, *Acc. Chem. Res.*, 2014, **47**, 2558; (*b*) W. T. Wu, L. Zhang and S. L. You, *Chem. Soc. Rev.*, 2016, **45**, 1570; (*c*) J. Liu, J. T. Chen, T. T. Liu, J. Liu and Y. F. Zeng, *Chin. J. Org. Chem.*, 2023, **43**, 379; (*d*) For selected examples, see: X. H. Liu, J. Y. Zhang, L. T. Bai, L. Q. Wang, D. X. Yang and R. Wang, *Chem. Sci.*, 2020, **11**, 671; (*e*) H. Egami, T. Rouno, T. Niwa, K. Masuda, K. Yamashita and Y. Hamashima, *Angew. Chem., Int. Ed.*, 2020, **59**, 14101; (*f*) B. G. Das, S. Shah, A. Das and V. K. Singh, *Org. Lett.*, 2021, **23**, 6262; (*g*) U. Maji, B. D. Mondal and J. Guin, *Org. Lett.*, 2023, **25**, 2323; (*h*) C. Parida, S. K. Dave, K. Das and S. C. Pan, *Adv. Synth. Catal.*, 2023, **365**, 1185.

6 For reviews, see: (*a*) R. Kumar, F. V. Singh, N. Takenaga and T. Dohi, *Chem.–Asian J.*, 2022, **17**, e202101115; (*b*) M. Okumura and D. Sarlah, *Eur. J. Org Chem.*, 2020, **10**, 1259; (*c*) X. Xiao and S. E. Wengryniuk, *Synlett*, 2021, **32**, 752; (*d*) For selected examples, see: Y. Wang, C. Y. Zhao, Y. P. Wang and W. H. Zheng, *Synthesis*, 2019, **51**, 3675; (*e*) H. L. Zheng, L. Cai, M. Pan, M. Uyanik, K. Ishihara and X. S. Xue, *J. Am. Chem. Soc.*, 2023, **145**, 7301; (*f*) A. H. Abazid and B. J. Nachtsheim, *Angew. Chem., Int. Ed.*, 2020, **59**, 1479; (*g*) M. Uyanik, S. Ishizaki and K. Ishihara, *Org. Synth.*, 2021, **98**, 1; (*h*) Y. Zhang, Y. T. Liao, X. H. Liu, X. Xu, L. L. Lin and X. M. Feng, *Chem. Sci.*, 2017, **8**, 6645.

7 For reviews, see: (*a*) J. Z. An and M. Bandini, *Eur. J. Org Chem.*, 2020, **27**, 4087; (*b*) U. K. Sharma, P. Ranjan, E. V. Van der Eycken and S. L. You, *Chem. Soc. Rev.*, 2020, **49**, 8721; (*c*) For selected examples, see: C. X. Zhou and S. L. You, *Angew. Chem., Int. Ed.*, 2013, **52**, 10056; (*d*) Z. P. Yang, Q. F. Wu and S. L. You, *Angew. Chem., Int. Ed.*, 2014, **53**, 6986; (*e*) X. J. Lian, L. L. Lin, G. J. Wang, X. H. Liu and X. M. Feng, *Chem.–Eur. J.*, 2015, **21**, 17453; (*f*) S. L. Ge, T. F. Kang, L. L. Lin, X. Y. Zhang, P. Zhao, X. H. Liu and X. M. Feng, *Chem. Commun.*, 2017, **53**, 11759; (*g*) Q. X. Zhang, Q. Gu and S. L. You, *Org. Lett.*, 2022, **24**, 8031; (*h*) R. Pedrazzani, J. An, M. Monari and M. Bandini, *Eur. J. Org Chem.*, 2021, **11**, 1732; (*i*) D. C. Wang, P. P. Cheng, T. T. Yang, P. P. Wu, G. R. Qu and H. M. Guo, *Org. Lett.*, 2021, **23**, 7865; (*j*) J. J. Hu, S. L. Pan, S. Zhu, P. Y. Yu, R. G. Xu, G. F. Zhong and X. F. Zeng, *J. Org. Chem.*, 2020, **85**, 7896; (*k*) B. M. Yang, X. J. Zhai, S. B. Feng, D. Y. Hu, Y. H. Deng and Z. H. Shao, *Org. Lett.*, 2019, **21**, 330; (*l*) Q. X. Zhang, J. H. Xie, Q. Gu and S. L. You, *Chem. Commun.*, 2023, **59**, 3590; (*m*) Y. L. Yu, Z. H. Zhang, A. Voituriez, N. Rabasso, G. Frison, A. Marinetti and X. Guinchard, *Chem. Commun.*, 2021, **57**, 10779; (*n*) L. B. Han, H. Wang and X. J. Luan, *Org. Chem. Front.*, 2018, **5**, 2453; (*o*) J. Zheng, S. B. Wang, C. Zheng and S. L. You, *J. Am. Chem. Soc.*, 2015, **137**, 4880.

8 (*a*) M. T. Peruzzi, S. J. Lee and M. R. Gagne, *Org. Lett.*, 2017, **19**, 6256; (*b*) S. L. Huang, L. Kötzner, C. K. De and B. List, *J. Am. Chem. Soc.*, 2015, **137**, 3446; (*c*) J. Z. An, A. Parodi, M. Monari, M. C. Reis, C. S. Lopez and M. Bandini, *Chem.–Eur. J.*, 2017, **23**, 17473; (*d*) L. Yao and K. Ishihara, *Chem. Sci.*, 2019, **10**, 2259; (*e*) A. S. Alshreimi, G. Q. Zhang, T. W. Reidl, R. L. Peña, N. G. Koto, S. M. Islam, D. J. Wink and L. L. Anderson, *Angew. Chem., Int. Ed.*, 2020, **59**, 15244.

9 For selected reviews of aromatic [*n*,*m*]-sigmatropic rearrangement, see: (*a*) K. Hiratani and M. Albrecht, *Chem. Soc. Rev.*, 2008, **37**, 2413; (*b*) Y. C. Liang and B. Peng, *Acc. Chem. Res.*, 2022, **55**, 2103; (*c*) Y. B. Liu, X. H. Liu and X. M. Feng, *Chem. Sci.*, 2022, **13**, 12290; (*d*) For selected examples, see: F. C. Gozzo, S. A. Fernandes, D. C. Rodrigues, M. N. Eberlin and A. J. Marsaioli, *J. Org. Chem.*, 2003, **68**, 5493; (*e*) H. Ito, A. Sato and T. Taguchi, *Tetrahedron Lett.*, 1997, **38**, 4815; (*f*) T. S. Castro, G. F. Martins, S. F. de Alcântara Morais and D. A. C. Ferreira, *Theor. Chem. Acc.*, 2023, **142**, 40; (*g*) T. R. Ramadhar, J. Kawakami, A. J. Lough and R. A. Batey, *Org. Lett.*, 2010, **12**, 4446; (*h*) L. Song, H. Yao and R. Tong, *Org. Lett.*, 2014, **16**, 3740; (*i*) C. K. Chan, Y. H. Chen, Y. L. Tsai and M. Y. Chang, *J. Org. Chem.*, 2017, **82**, 3317; (*j*) T. Abe, Y. Kosaka, M. Asano, N. Harasawa, A. Mishina, M. Nagasue, Y. Sugimoto, K. Katakawa, S. Sueki, M. Anada and K. Yamada, *Org. Lett.*, 2019, **21**, 826; (*k*) L. Yao, K. Takeda, K. Ando and K. Ishihara, *Chem. Sci.*, 2023, **14**, 2441.

10 J. Z. An, A. Parodi, M. Monari, M. C. Reis, C. S. Lopez and M. Bandini, *Chem.–Eur. J.*, 2017, **23**, 17473.

11 L. F. Wang, Y. Q. Zhou, Z. S. Su, F. C. Zhang, W. D. Cao, X. H. Liu and X. M. Feng, *Angew. Chem., Int. Ed.*, 2022, **61**, e202211785.
12 L. Yao and K. Ishihara, *Chem. Sci.*, 2019, **10**, 2259.
13 For examples about the π-complex mechanism, see: (*a*) M. J. S. Dewar, *The Electronic Theory of Organic Chemistry*, Oxford University Press, London, 1949, p. 229; (*b*) D. Y. Curtin and H. W. Johnson Jr, *J. Am. Chem. Soc.*, 1956, **78**, 2611; (*c*) J. Borgulya, R. Madeja, P. Fahrni, H. J. Hansen, H. Schmid and R. Barner, *Helv. Chim. Acta*, 1973, **56**, 14; (*d*) X. G. Lei, M. J. Dai, Z. H. Hua and S. J. Danishefsky, *Tetrahedron Lett.*, 2008, **49**, 6383.
14 For selected examples of *para*-Claisen rearrangements, see: (*a*) J. P. Ryan and P. R. O'Connor, *J. Am. Chem. Soc.*, 1952, **74**, 5866; (*b*) K. Maruoka, J. Sato, H. Banno and H. Yamamoto, *Tetrahedron Lett.*, 1990, **31**, 377; (*c*) Y. Okada and D. Imanari, *Int. J. Org. Chem.*, 2012, **2**, 38; (*d*) Z. Hui, S. W. Jiang, X. Qi, X. Y. Ye and T. Xie, *Tetrahedron Lett.*, 2020, **61**, 151995; (*e*) F. Salahi, C. B. Yao, J. R. Norton and S. A. Snyder, *Nat. Synth.*, 2022, **1**, 313; (*f*) J. A. Homer, I. D. Silvestro, E. J. Matheson, J. T. Stuart and A. L. Lawrence, *Org. Lett.*, 2021, **23**, 3248.
15 For selected reviews of *N*,*N*′-dioxide/metal catalysis, see: (*a*) H. X. Liu, L. L. Lin and X. M. Feng, *Org. Chem. Front.*, 2014, **1**, 298; (*b*) M. Y. Wang and W. Li, *Chin. J. Chem.*, 2021, **39**, 969; (*c*) W. D. Cao, X. H. Liu and X. M. Feng, *Chin. Sci. Bull.*, 2020, **65**, 2941; (*d*) D. F. Chen and L. Z. Gong, *Org. Chem. Front.*, 2023, **10**, 3676; (*e*) X. H. Liu, L. L. Lin and X. M. Feng, *Acc. Chem. Res.*, 2011, **44**, 574; (*f*) X. H. Liu, H. F. Zheng, Y. Xia, L. L. Lin and X. M. Feng, *Acc. Chem. Res.*, 2017, **50**, 2621; (*g*) X. H. Liu, S. X. Dong, L. L. Lin and X. M. Feng, *Chin. J. Chem.*, 2018, **36**, 791; (*h*) For selected examples, see: T. Y. Zhan, L. K. Yang, Q. Y. Chen, R. Weng, X. H. Liu and X. M. Feng, *CCS Chem.*, 2023, **5**, 2101; (*i*) K. X. Wang, L. Q. Yang, Y. Li, Z. L. Liu, L. C. Ning, X. H. Liu and X. M. Feng, *Angew. Chem., Int. Ed.*, 2023, **62**, e202307249; (*j*) Q. W. He, M. P. Pu, Z. Jang, H. Y. Wang, X. M. Feng and X. H. Liu, *J. Am. Chem. Soc.*, 2023, **145**, 15611.
16 For the X-ray crystal structure of the *N*,*N*′-dioxide/Co(II) complex: W. Yang, M. P. Pu, X. B. Lin, M. Chen, Y. J. Song, X. H. Liu, Y. D. Wu and X. M. Feng, *J. Am. Chem. Soc.*, 2021, **143**, 9648.